Reversible formation of soft coordination polymers from liquid mixtures of photoreactive organometallic ionic liquid and bridging molecules

Sumitani, Ryo

Mochida, Tomoyuki

(Citation)
Soft Matter,16(43):9946-9954

(Issue Date)
2020-11-21

(Resource Type)
journal article

(Version)
Accepted Manuscript

(URL)
https://hdl.handle.net/20.500.14094/90007639

Reversible Formation of Soft Coordination Polymers from Liquid Mixtures of Photoreactive Organometallic Ionic Liquid and Bridging Molecules†

Ryo Sumitani,[a] Tomoyuki Mochida*[ab]

The reversible switching of bonding modes in coordination polymers through the application of external stimuli leads to versatile mechanical and electronic functions. However, the exploration of such a system remains a great challenge. In this study, we designed liquid mixtures comprising a photoreactive organometallic ionic liquid and a bridging ligand, which form intermolecular coordination bonds upon photoirradiation. The liquid mixture of an ionic liquid $[Ru(C_5H_5)\{Ph(CH_2)_3CN\}][(SO_2F)_2N]$ (**1**) and a tridentate ligand $N(C_2H_4CN)_3$ was transformed into an elastomer of an amorphous coordination polymer upon ultraviolet photoirradiation. By contrast, the photoirradiation of the mixture of **1** and a bidentate ligand $NC(CH_2)_4CN$ produced a highly viscous liquid comprising coordination-bonded oligomers. In these reactions, photoirradiation causes dissociation of the organometallic cation, followed by the formation of intermolecular coordination bonds via the bridging ligands. The photoproducts underwent reverse reactions thermally. Based on coordination transformation, the ionic conductivity and viscoelasticity of these materials were reversibly controlled by the application of light and heat.

Introduction

Recently, organic polymers with dynamic covalent bonds or supramolecular interactions, which reversibly dissociate by external stimuli such as heat, have attracted considerable attention because of their self-healing properties.[1–5] Some polymers exhibit reversible changes in their physical properties (such as viscoelasticity and ionic conductivity) as a result of external stimuli based on the reversible bond formation mechanisms.[6,7] These features are useful for sensors and electronic devices. Coordination bonds are also useful for bonding transformations. There are stimuli-responsive metallopolymers that exhibit reversible bond formation.[8–14] However, metallopolymers mostly have low-dimensional structures,[15] and there are very few examples of coordination polymers with this property.[16] This is partly because coordination polymers are generally crystalline, hard materials.[15,17]

To explore stimuli-responsive network coordination polymers, we recently designed soft coordination polymers that are produced by the photoirradiation of metal-containing ionic liquids.[18–21] Ionic liquids are salts with melting points below 100 °C.[22] For example, the Ru-containing ionic liquid (***tri*-1**) shown in Fig. 1a transforms into an amorphous coordination polymer (***tri*-2**) upon UV photoirradiation.[18] Heating the solid product causes a reverse reaction into the ionic liquid, thereby enabling the reversible formation of coordination polymers through the application of light and heat. In this reaction, photoirradiation causes dissociation of the arene ligand, followed by the coordination of three cyano groups from the ligand to form a network structure. Furthermore, this feature enables the reversible control of its ionic conductivity and viscoelasticity.[19]

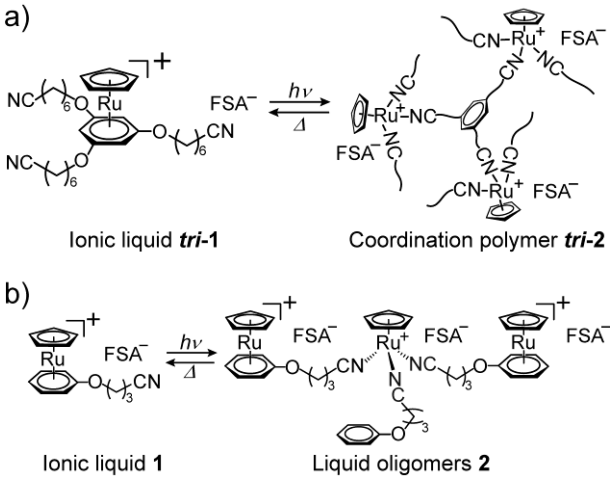

Fig. 1. Reversible formation of (a) coordination polymer and (b) oligomer liquid from ruthenium-containing ionic liquids. FSA^- stands for bis(fluorosulfonyl)amide anion.

Although this salt has a versatile material design through which it can reversibly control physical properties via external stimuli, its photoreaction requires several hours under standard ultraviolet (UV) light-emitting diode (LED) light. To overcome this disadvantage, we further designed a photoreactive ionic liquid $[Ru(C_5H_5)(PhOC_3H_6CN)][FSA]$ (**1**) with only one substituent (Fig. 1b).[19] Its photoreaction is more than 10× faster than that shown in Fig. 1a because of its low viscosity. However, the product is a liquid composed of trinuclear complexes, and no photo solidification occurs.

The purpose of this study is to design a novel type of photoreactive liquid that transforms into a solid coordination polymer upon photoirradiation, while maintaining high reactivity. The idea was to

[a]*Department of Chemistry, Graduate School of Science, Kobe University, 1-1 Rokkodai, Nada, Kobe, Hyogo 657-8501, Japan.*
E-mail: tmochida@platinum.kobe-u.ac.jp
[b]*Center for Membrane Technology, Kobe University, 1-1 Rokkodai, Nada, Kobe, Hyogo 657-8501, Japan*
†Electronic Supplementary Information (ESI) available: NMR, FT-IR, and UV-Vis spectra and DSC traces.. See DOI: 10.1039/x0xx00000x

add a tridentate bridging ligand to **1**, as schematically illustrated in Fig. 2a. Photoirradiation of the liquid mixture would produce a network coordination polymer linked by the tridentate ligands, whereas the low viscosity of the liquid mixtures enables fast reactions. By contrast, the use of a bidentate ligand instead of a tridentate ligand would produce a one-dimensional structure or oligomers (Fig. 2b), which are less likely to form a solid.

Based on this idea, in this study, we prepared liquid mixtures of ionic liquid **1** and the bridging ligands shown in Fig. 3 and investigated their thermal properties and photoreactivities. The tridentate ligand tris(2-cyanoethyl)amine ($N(C_2H_4CN)_3$, **L**) and bidentate ligand 1,4-dicyanobutane ($NC(CH_2)_4CN$, **L'**) both have high boiling points and low vapor pressures. As shown below, the liquid mixture of **1** and **L** (abbreviated as **1a**, hereafter) transformed into soft amorphous coordination polymer **2a** upon UV photoirradiation (Fig. 4), whereas the mixture of **1** and **L'** (abbreviated as **1b**) transformed into oligomer liquid **2b** (Fig. 5). These photoreaction products reverted to the original liquids upon heating. Their ionic conductivity and viscoelasticity changes upon photoirradiation were investigated and are discussed compared with those of related Ru-containing ionic liquids.

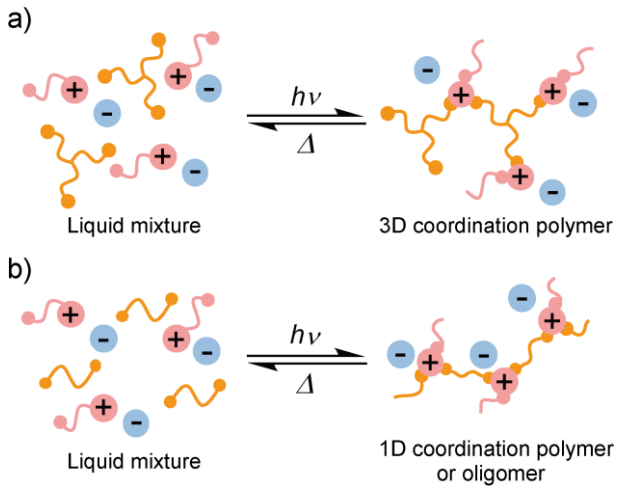

Fig. 2. Schematic illustration of photochemical reactions of liquid mixtures comprising photoreactive ionic liquid and (a) tridentate or (b) bidentate bridging ligand.

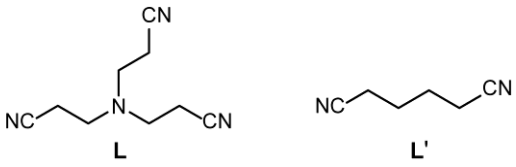

Fig. 3. Bridging ligands used in this study.

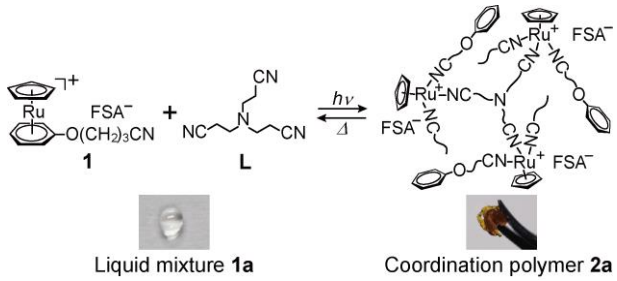

Fig. 4. Photochemical transformation of liquid mixture **1a** into soft amorphous coordination polymer **2a**. The product contains some unreacted cations inside the solid. Reverse reaction occurs thermally. Photographs before and after UV irradiation are shown below each formula.

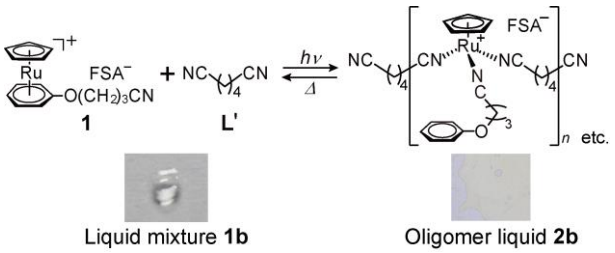

Fig. 5. Photochemical transformation of **1b** into oligomer liquid **2b**. Product contains some unreacted cations and other oligomeric species. Reverse reaction occurs thermally. Photographs before and after UV irradiation are shown below each formula, wherein **2b** is sandwiched between two quartz plates.

Experimental

General

Ionic liquid **1** was synthesized according to the method in the literature.[23] ^1H and ^{19}F nuclear magnetic resonance (NMR) spectra were recorded using a Bruker Avance 400 spectrometer. The infrared (IR) spectra were recorded using a Thermo Nicolet iS5 instrument with an attenuated total reflection attachment. The ultraviolet–visible (UV–vis) spectra were measured using a JASCO V-570 UV/VIS/NIR spectrophotometer. Differential scanning calorimetry (DSC) measurements were performed using a TA Instruments Q100 differential scanning calorimeter with a sweep rate of 10 K min^{-1}. ESI-MS spectra were measured using a Thermo Fisher Scientific LTQ-Orbitrap Discovery. The viscosity of the liquids was measured using a TA Instruments Discovery HR-1. The ionic conductivities were measured using a Solartron 1260 impedance analyzer and gold interdigitated electrodes with gap dimensions of 200 μm. Since repeated photo and thermal reactions in air cause gradual oxidation of the ruthenium complex,[20] the samples were sandwiched between the electrode and a quartz glass plate and further coated with epoxy resin.

Photoreaction

To prepare **1a** and **1b**, ionic liquid **1** and the corresponding bridging ligand were mixed at a molar ratio of 3:2 and 1:1, respectively, in dichloromethane. After irradiation with ultrasonic waves for 5 min, the solvent was evaporated under reduced pressure, and the residue was vacuum dried at ambient temperature for 1 h. The compositions of the resultant liquids were checked by ^1H NMR spectroscopy in

CD_3CN. To investigate the photoreaction, UV light was irradiated into the liquids sandwiched between two quartz plates at 10 °C. A Lightningcure UV-LED spotlight source (LC-L1V5, Hamamatsu Photonics; 365 nm, 600 mW cm^{-2}) was used as the light source. For the viscoelastic measurements, the photoreaction was slower owing to the increased sample thickness (15–35 μm).

Result and discussion

Thermal properties and photoreactivity

For the preparation of **1a** and **1b**, **1** and the corresponding bridging ligands were mixed in molar ratios of 3:2 and 1:1, respectively. The ratios were set such that the ratio of ruthenium to cyano groups was 1:3, considering the reaction mechanism.

Upon UV photoirradiation, colorless liquids **1a** and **1b** transformed into soft yellow elastomer **2a** and yellow highly viscous liquid **2b**, respectively, after 30 min (Figs. 4 and 5). The products contained ~20% unreacted cations. The products reverted to the original colorless liquid mixtures upon heating, although the thermal reaction occurred slowly even at ambient temperature. Details of the reactions are described in the following sections.

The thermal properties of the liquid mixtures and photoproducts were investigated using DSC. The glass transition temperatures and melting points of the compounds are summarized in Table 1. The DSC traces are shown in Fig. 6. **1a** and **1b** did not solidify upon cooling, exhibiting glass transitions at T_g = −70 °C and −84 °C, respectively. Their glass transition temperatures are lower than that of **1** (T_g = −60 °C),[23] which is ascribed to the decrease in viscosity due to the addition of bridging ligands. The melting points of **L** and **L'** are 59 °C and 1.9 °C, respectively,[24,25] exhibiting crystallization upon cooling, whereas **L** additionally exhibits a solid phase transition. Therefore, the observation of only a glass transition in the liquid mixtures indicates their homogeneity and no phase separation. An ionic liquid with a longer substituent $[Ru(C_5H_5)(PhOC_6H_{12}CN)][FSA]$ (T_m = 43.5 °C)[23] was less useful because its mixtures with the bridging ligands exhibited partial solidification at ambient temperature. The photoreaction products **2a** and **2b** exhibited glass transitions at T_g = −26 °C and −40 °C, respectively. These glass transition temperatures, which are considerably higher than those of **1a** and **1b,** are consistent with the formation of intermolecular coordination bonds. The thermal behaviours of the photoproducts are discussed in the following sections.

Table 1 Glass transition temperatures (T_g) and melting points (T_m) of liquid mixtures, their photoproducts, ionic liquid, and bridging ligands

Compounds		T_g [°C]	T_m [°C]
Liquid mixture	**1a**	−70	
	1b	−80	
Photoproduct	**2a** (74%)[a]	−26	
	2b (63%)[a]	−40	
Ionic liquid	**1**	−60 [b]	
Bridging ligand	**L**		59 [c]
	L'		1.9 [d]

[a] Reaction rate. [b] Ref. 23. [c] Ref. 24. [d] Ref. 25.

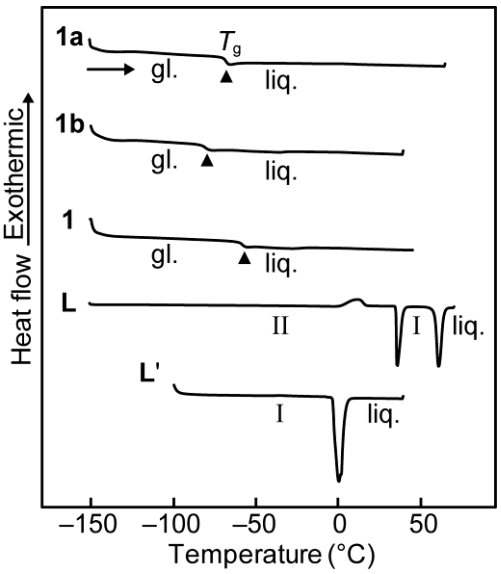

Fig. 6. DSC traces of **1a**, **1b**, **1**, **L**, and **L'** recorded on heating runs (gl.: glassy phase, liq.: liquid phase, I, II: crystal phases, ▲ : glass transition).

Investigation of photochemical reactions

The photochemical reactions and reverse reactions of **1a** and **1b** were investigated by ^1H NMR, UV-vis, and IR spectroscopy. Their spectral changes were similar to those of ***tri*-1** (Fig. 1a).[18] As shown in Figs. 4 and 5, photoirradiation of the liquids caused photodissociation of the sandwich complex, followed by coordination of the cyano groups from the bridging ligands.

The ^1H NMR spectra of **1a** and its photoproduct **2a,** measured in CD_3CN, are shown in Fig. 7. The coordination polymer component in **2a** dissociates in CD_3CN to yield a mixture of a solvent-coordinated complex $[Ru(C_5H_5)(CD_3CN)_3]^+$ (80%) and free ligands (Fig. 7b); the unreacted sandwich complex $[Ru(C_5H_5)(PhO(CH_2)_3CN)]^+$ (20%) was also observed. The data indicate that the reaction rate was 80%, and the presence of unreacted cations in the product may be ascribed to the incorporation of the cation into the network structure during the photoreaction, as similarly observed in the photoreaction of ***tri*-1**.[18] Another possibility is the concomitant thermal reverse reaction during photoirradiation.

Heating the coordination polymer completely recovered the original liquid (Fig. 7c). The structural change was also supported by the UV-vis and IR spectra. **1a** had no absorption bands in the visible region, but the absorption bands characteristic of the cyano coordinated complex appeared at λ_{max} = 310 and 370 nm after photoirradiation (Fig. 8a),[18,26] which is consistent with the color change from colorless to yellow. Similarly, the CN stretching peaks in

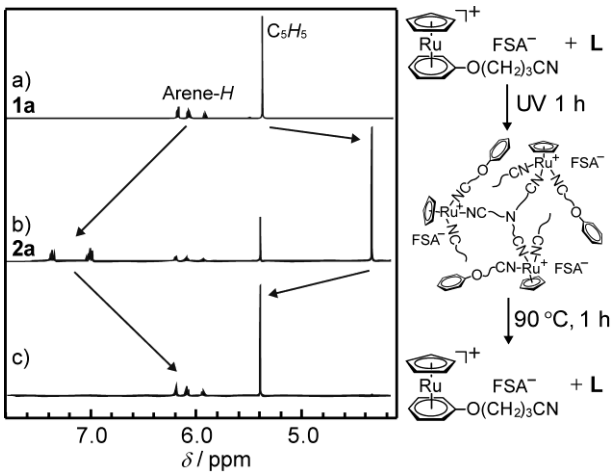

Fig. 7. ^{1}H NMR spectra of (a) **1a**, (b) **2a**, and (c) after heating **2a** at 90 °C for 1 h (CD_3CN). Coordination polymer dissociates to yield an acetonitrile-coordinated species when dissolved in CD_3CN.

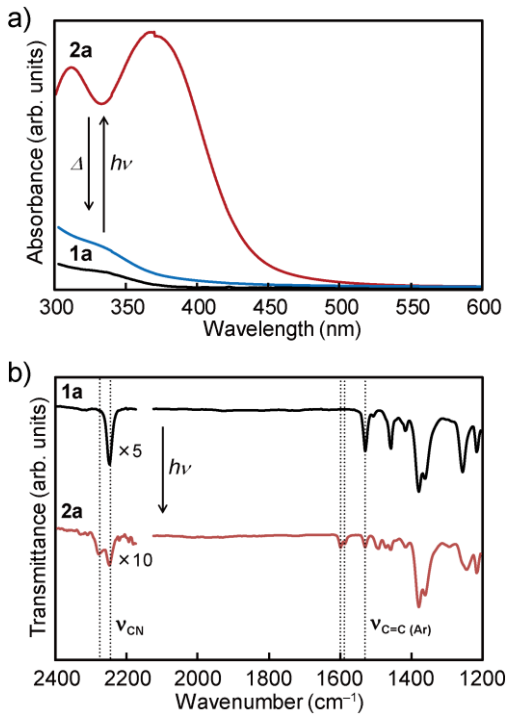

Fig 8. (a) UV-vis and (b) IR spectra of **1a** and **2a**.

the IR spectrum shifted from 2243 cm^{-1} to 2270 cm^{-1} after photoirradiation (Fig. 8b), which corresponds to the change from the non-coordinating to metal-coordinated cyano group.[18] The C=C stretching peaks of the arene ligand shifted from 1530 cm^{-1} to 1584 and 1599 cm^{-1}, which corresponds to the change from a coordinated to non-coordinated ligand.[18] These spectral changes were reversible by the application of light and heat. The absorbance change in the UV spectra shown in Fig. 8a is ascribed to different sample thicknesses.

The thermal behavior of **2a**, as revealed by DSC, was consistent with its thermal reactivity. The DSC traces of **2a** (reaction rate 74%) are shown in Fig. 9, which exhibits a glass transition at –26 °C (cycle

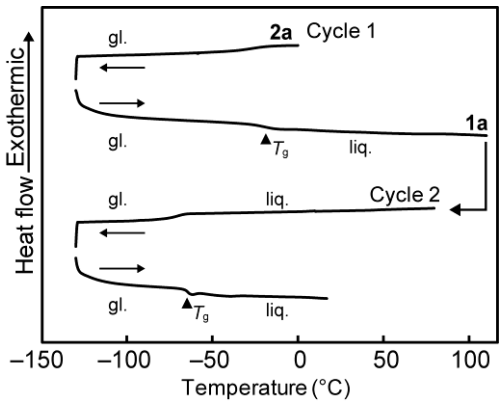

Fig. 9. DSC traces of **2a** (gl.: glassy phase, liq.: liquid phase).

1). Upon heating in cycle 1, a very broad, small endothermic peak was observed at approximately 60 °C (not clearly visible in the figure). The peak probably corresponds to the coordination transformation, similar to the case of ***tri*-2**, which displayed a broad peak at approximately 100 °C.[18] In the second cycle, a glass transition was observed at −70 °C, which is consistent with the transformation into **1a**.

1b exhibited similar spectral changes upon photoirradiation (Figs. S1-S3, ESI†). The product contained unreacted cations of approximately 25%, as determined from the ^{1}H NMR spectrum. The presence of the unreacted cation may be due to the concomitant thermal reverse reaction during photoirradiation. The product was an equilibrium mixture of coordination-bonded oligomers, and the dominant species may be trimer or tetramer, considering the amount of unreacted cations. However, it was impossible to identify each component spectroscopically owing to the lability of the coordination bond. The thermal transformation from **2b** (T_g = −40 °C) to **1b** was also confirmed by DSC measurements, in which the glass transition of **1b** (T_g = −78 °C) was observed in the second cycle (Fig. S3, ESI†). During the heating process in cycle 1, a very broad endothermic peak was observed at approximately 40 °C, which corresponds to the coordination transformation.

The contrasting photoproducts of **1a** and **1b**, which are solid and liquid, respectively, are reasonable in terms of dimensionality. One-dimensional systems are susceptible to defects to form oligomers, whereas two- and three-dimensional systems maintain their network structures, despite the defects resulting from the presence of unreacted cations.

Rates of photochemical and thermal reactions

The photoreaction rates of **1a** and **1b** were investigated in detail. The rates of photodissociated cations in their reactions are plotted as a function of photoirradiation time in Fig. 10, together with those of **1** and ***tri*-1**.[18,19] The plots show that the reaction rates of **1a** and **1b** were almost constant over 0.5 h at 80% and 75%, respectively. The photoreactions of **1a** and **1b** were more than 10× faster than that of ***tri*-1**. The reaction rates of **1a** and **1b** reached 50% in 10 min, whereas it took 100 min for ***tri*-1**. The reactions were, however, somewhat slower than that of **1**, which reached a constant value (31%) within 15 min. It should be noted that the dissociation rate of 31% in **1**

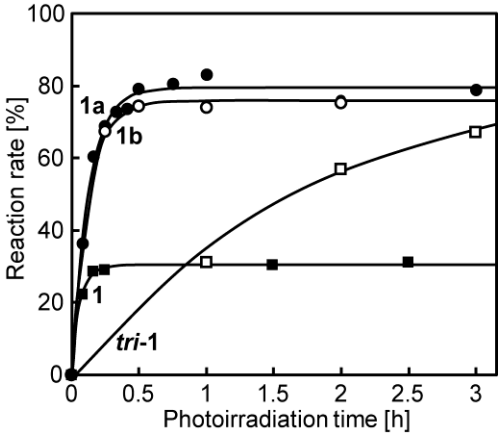

Fig. 10. Photoreaction rates of **1a** (●) and **1b** (○) plotted versus photoirradiation time as determined from the UV-vis spectral absorbance at 370 nm and ^{1}H NMR spectra. The data for **1** (■) and ***tri*-1** (□) are also shown.

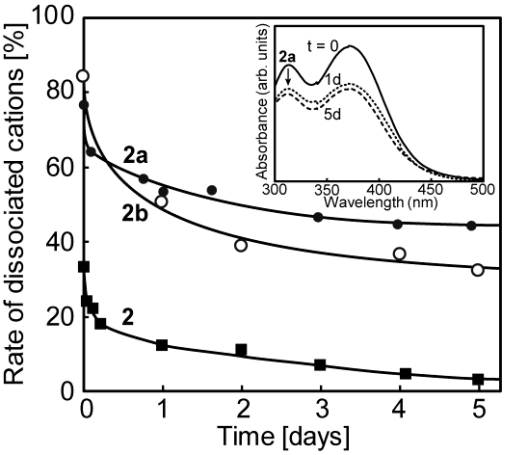

Fig. 11. Time course of rate of dissociated cations in **2a** (●), **2b** (○), and **2** (■) when left at 17 °C under dark as determined from the UV-vis spectral absorbance at 370 nm and ^{1}H NMR spectra. Inset shows change in UV-vis spectra of **2b**.

corresponds to a 93% overall reaction rate because the dominant product is a trimer containing two undissociated cations.[19] It is noteworthy that the reaction of **1a** is fast despite its transformation into a solid.

Both **2a** and **2b** underwent reverse reactions upon heating at 100 °C for a few minutes, when complete transformation into original **1a** and **1b** was observed. However, the reaction occurred slowly even at ambient temperature. This is consistent with the observation of the DSC peaks owing to the coordination transformation near room temperature. The time course of the rate of dissociated cations in **2a** and **2b** when left at 17 °C is shown in Fig. 11. The rate decreased to 44% (**2a**) and 33% (**2b**) after 5 days. This feature indicates that **2a** retains the intermolecular coordination bonds for a longer time than **2b** does, which is consistent with the results of the DSC measurements. Their facile thermal reverse reaction is partly ascribed to the effect of entropy, which makes the original liquid mixtures more favorable energetically. The dissociation rate in **2** decreased from 33% to 2% over 5 d, whereas the dissociation was very slow in the dichloromethane solution.[19] These results are in contrast to ***tri*-2**, for which the reverse reaction was not noticeable at ambient temperature. This is consistent with the higher coordination transformation temperature of ***tri*-2** (~100 °C) than that of **2a** and **2b**.[18]

Viscoelasticity

Dynamic viscoelasticity measurements were taken at 25 °C to evaluate the changes in the physical properties of **1a** and **1b** upon photoirradiation. The samples after the photoirradiation of **1a** for 18 h (67% reaction rate) and **1b** for 8.3 h (61% reaction rate) are designated as **2a** and **2b**, respectively. Their reaction rates were lower than those reported in the previous sections because the samples were thicker. Photoirradiation caused a marked increase in the elastic modulus and viscosity owing to the structural transformations.

The viscosity and complex viscosity data before and after photoirradiation are summarized in Table 2. The viscosities of **1a** and **1b** were 620 mPa·s and 89 mPa·s, respectively, at a shear rate of 1 s^{-1}. Their viscosities were considerably lower than that of **1** (920 mPa·s, at 1 s^{-1}). In particular, the viscosity of **1b** is one order of magnitude smaller than that of **1a** and even closer to that of a typical ionic liquid [Emim][FSA] (Emim = 1-ethyl-3-methylimidazolium cation; 19 mPa·s, at 20 °C).[27] Although Ru-containing organometallic ionic liquids are generally highly viscous, the results demonstrate that mixing additional molecules is an effective method for reducing their viscosity.

The angular frequency (ω) dependence of the storage and loss elastic modulus of **1a** measured after photoirradiation for 0.5 h, 10 h, and 18 h (**2a**) are shown in Fig. 12a. Initially, the loss elastic modulus exceeds the storage elastic modulus in the entire frequency range. However, both the storage and loss elastic modulus increased by three to four orders of magnitude with photoirradiation time, and the storage elastic modulus exceeded the loss elastic modulus in the frequency region at $\omega > 16$ rad s^{-1} in 10 h and $\omega > 2$ rad s^{-1} in 18 h. The time course of the storage elastic modulus and loss tan δ (= G' / G'') of **1a** measured upon photoirradiation (angular frequency 10 rad s^{-1}) is shown in Fig. 12b. The loss tan δ approached 1 in 6 h, indicating a semi-solid property. However, the loss elastic modulus was still large and tan δ was not much smaller than 1 even after 18 h of photoirradiation, which is ascribed to the presence of 33% of unreacted cations. These features demonstrate the transformation from liquid into a rubbery elastomer. The complex viscosities of **1a** before and after photoirradiation are shown in Fig. 12c. The values for **1a** and **2a** were 4.8×10^2 and 6.7×10^7 mPa·s at an angular frequency of 10 rad s^{-1}, and increased by five orders of magnitude upon photoirradiation.

The viscosity of **1b** before and after photoirradiation for 0.2 h, 1.0 h, and 8.3 h (**2b**) are shown in Fig. 13. The viscosity increased with photoirradiation time, reflecting the transformation into oligomers. The viscosity of **2b** was 5.2×10^4 mPa·s at a shear rate of 1 s^{-1}, which was three orders of magnitude higher than that before

Table 2 Viscosity, ionic conductivity, and Walden product of **1a**, **1b**, and related materials at 25 °C

Compounds	Viscosity (mPa s)[a]		Ionic conductivity (S cm^{-1})		Walden product[d]
	Before[b]	After	Before	After[c]	(mPa s mS cm^{-1})
1a	6.2×10^2	6.7×10^7 [f] (67%)[g]	2.7×10^{-4}	8.7×10^{-6}	160
1b	8.9×10^1	5.2×10^4 [b] (61%)[g]	9.8×10^{-4}	2.0×10^{-5}	87
1[e]	9.2×10^2	5.2×10^3 [b] (28%)[g]	4.0×10^{-4}	3.2×10^{-5}	370
***tri*-1**[e]	2.6×10^3	1.2×10^8 [f] (84%)[g]	3.1×10^{-5}	3.2×10^{-6}	81

[a] 1 mPa s = 1 cP. [b] Value at a shear rate of 1 s^{-1}. [c] After 30 min photoirradiation. [d] Value before photoirradiation. [e] Ref. 19. [f] Complex viscosity at 10 rad s^{-1}. [g] Rate of dissociated cations.

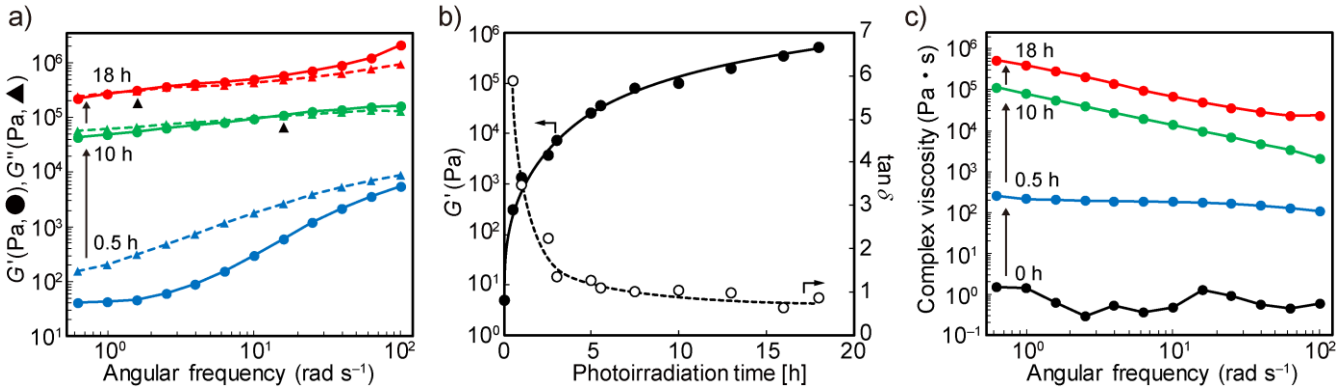

Fig. 12. (a) Storage elastic modulus (G', solid lines) and loss elastic modulus (G'', dashed lines) of **1a** after photoirradiation plotted as function of angular frequency. Data after photoirradiation for 0.5 h (blue), 10 h (green), and 18 h (red) are shown. Triangles indicate crossover points. (b) Storage elastic modulus (G', ●) and loss tan δ (○) of **1a** plotted versus photoirradiation time (25 °C, angular frequency 10 rad s^{-1}). (c) Complex viscosity of **1a** plotted as function of angular frequency measured before and after photoirradiation for 0.5 h, 10 h, and 18 h (1% strain).

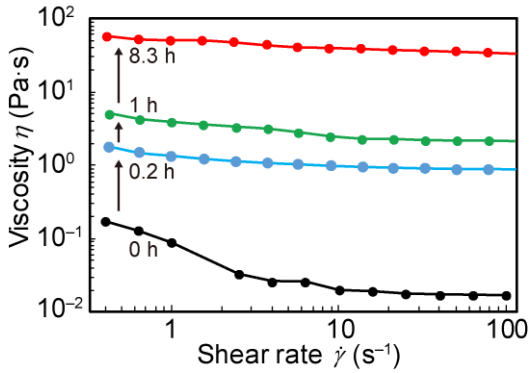

Fig. 13. Viscosity of **1b** plotted as function of shear rate at 25 °C measured before and after photoirradiation for 0.2 h, 1.0 h, and 8.3 h.

photoirradiation. The loss elastic modulus exceeded the storage elastic modulus in the entire frequency range, supporting its liquid state.

Ionic conductivities

The photoreaction of these liquid mixtures accompanies the formation of intermolecular coordination bonds, making the cation less mobile. Based on this mechanism, their ionic conductivities were reversibly controlled by the application of light and heat. The ionic conductivities of **1a** and **1b** before and after photoirradiation for 30 min are summarized in Table 2, together with those of **1** and ***tri*-1**.

The ionic conductivities of **1a** and **1b** before photoirradiation were 2.7×10^{-4} and 9.8×10^{-4} S cm^{-1}, respectively, which are similar to that of **1** (4.0×10^{-4} S cm^{-1}). The addition of bridging ligands lowers the ionic concentration, although it is compensated for by the decrease in viscosity. The Walden products, the products of ionic conductivity and solution viscosity, of these liquids were 160 and 87 mPa s mS cm^{-1}, respectively, which are considerably smaller than that of **1** (370 mPa s mS cm^{-1}).

The UV photoirradiation of **1a** reduced the ionic conductivity from 2.7×10^{-4} S cm^{-1} to 8.7×10^{-6} S cm^{-1} in 30 min owing to the transformation into a coordination polymer (Fig. 14a). The different photoreaction rates for the ionic conductivity and viscoelasticity measurements of **1a** are ascribed to different sample thicknesses. The similarity of their trends (Figs. 12b and 14a) indicates that they are both resulting from the network formation reaction. Subsequent heating at 120 °C for 20 min increased the value to 9.6×10^{-5} S cm^{-1} owing to the recovery of the liquid state. The ionic conductivity response of **1b** was similar to that of **1**,[19] exhibiting a smaller change than **1a** (Fig. 14a). The conductivity decreased upon UV photoirradiation from 9.8×10^{-4} S cm^{-1} to 2.0×10^{-5} S cm^{-1} in 30 min. Subsequent heating at 120 °C for 10 min increased the value to 9.1 ×

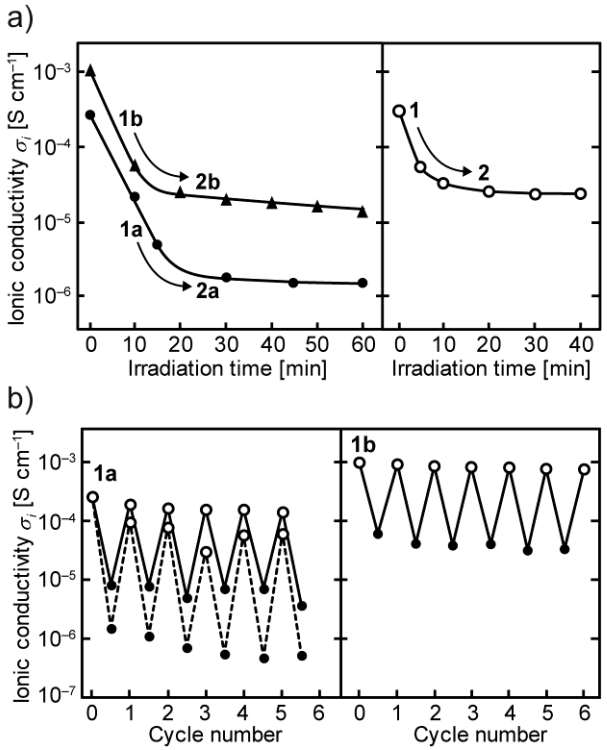

Fig. 14. (a) Time course of ionic conductivity of **1a** (●), **1b** (▲) and **1** (○) measured upon photoirradiation at 25 °C. (b) Ionic conductivity changes of **1a** and **1b** for alternating 10 min (—) or hourly (---) cycles of UV photoirradiation (filled circles) and 120 °C heating (open circles).

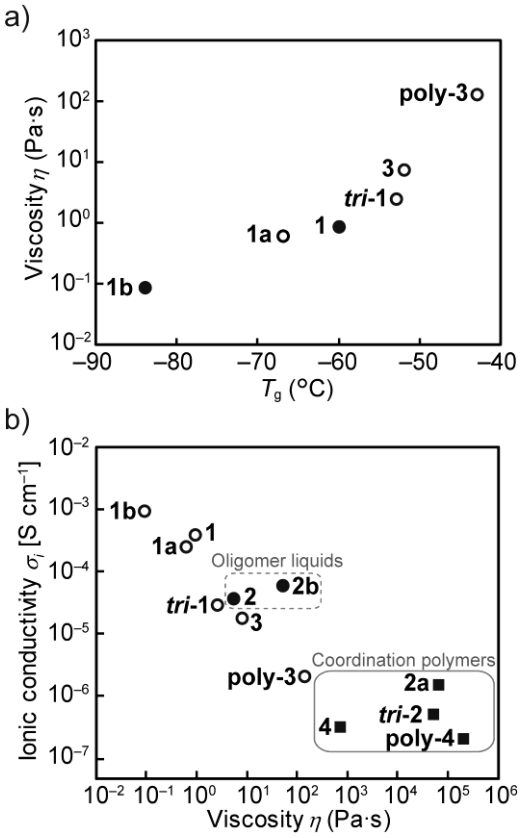

Fig. 15. (a) Correlation between glass transition temperature (T_g) and viscosity of liquid mixtures (**1a**, **1b**), ionic liquids[19,23] (**1**, **tri-1**, **3**), and poly(ionic liquid[20] (**poly-3**). (b) Correlation between viscosity and ionic conductivity. Values of viscosities and complex viscosities are plotted for liquids (○: before photoreaction, ●: oligomer liquids) and coordination polymers (■), respectively. Data for $[Ru(C_5H_5)\{C_6H_3(OC_6H_{12}CN)_3\}][H_2C{=}CHSO_2N^-SO_2CF_3]$ (**3**), its polymer (**poly-3**), and their photoproducts (**4** and **poly-4**) are also shown.

10^{-4} S cm^{-1}.

The reversible cycles of ionic conductivity in **1a** and **1b** are shown in Fig. 14b. These figures show the plot for alternating 10 min cycles of UV photoirradiation and 120 °C heating. For **1a**, the conductivity for alternating hourly cycles is also shown, which exhibits a larger change (Fig. 14b left, dotted line). Repeating the cycle of photo and thermal reactions of **1a** and **1b** resulted in a very slight decrease in ionic conductivity, which could be due to slight oxidation of the sample or contamination by epoxy resin from the sample holder. It is noteworthy that the current liquids exhibit a fast response comparable to **1**, and in particular, **1a** exhibits a large ionic conductivity change upon photoirradiation, as seen in Fig. 14a. These features are potentially useful for device applications.

Correlation of viscosity, glass transition temperature, and ionic conductivity

In this section, we discuss physical property changes before and after the photoreaction of the current and related materials that have the same bond-switching mechanism. The viscosities of **1**, **1a**, **1b**, ***tri*-1**, and related materials ($[$***tri*-1**$][H_2C{=}CHSO_2NSO_2CF_3]$ (**3**) and the corresponding poly(ionic liquid) (**poly-3**)[20]) are plotted versus their glass transition temperatures in Fig. 15a. The viscosity increases with the increase in the glass transition temperature, including data for **1a**, **1b**, and **poly-3**, which are not genuine ionic liquids. The ionic conductivities before and after UV photoirradiation are plotted against the viscosity and complex viscosity in Fig. 15b. The values of viscosities and complex viscosities are plotted for liquids and elastomers, respectively, which are nearly equivalent according to the empirical Cox–Merz rule.[28] Before photoirradiation, the ionic conductivities of liquids with lower viscosity tend to be larger (**1b** > **1a** ≈ **1** > ***tri*-1** > **3** > **poly-3**), as is generally observed in ionic liquids.[29,30] The changes in viscosity and ionic conductivity before and after the photoreaction are small during the transformation into oligomer liquids (**2** and **2b**), whereas the changes are generally large during the transformation into three-dimensional coordination polymers. This figure also shows that Ru-containing ionic liquids can be used to create materials with a wide range of ionic conductivities and viscoelastic properties.

These studies demonstrate the versatility of the coordination-bond switching mechanism of external stimuli in controlling their physical properties. Ru-containing organometallic complexes will have versatile applications in the further development of functional soft coordination compounds, since they are also useful for the controlled construction of dendrimers.[31]

Conclusions

In this study, as a novel approach to fabricating soft coordination polymers from liquids, we designed photoreactive liquid mixtures comprising a Ru-containing ionic liquid and a bridging molecule. The liquid mixtures produced an amorphous network coordination polymer or oligomer liquid upon photoirradiation. The use of different bridging ligands, either tridentate or bidentate, changed the topology and fluidity of the products. In addition, the liquid mixtures had lower viscosity than the ionic liquid component, enabling rapid photoreaction. The liquid design is advantageous for materials variation. Furthermore, based on the reversible coordination transformation by the application of light and heat, their ionic conductivities and viscoelastic properties were reversibly controlled. The comparison of the current and related materials proved the coordination-bond switching mechanism useful for controlling their physical properties over a wide range. Their tunable ionic conductivity and viscoelastic properties may be useful for future device applications. The mechanical and self-healing properties of these materials are worthy of future investigation.

Conflicts of interest

There are no conflicts to declare.

Acknowledgements

We thank Takuya Kusakabe for his help with the preparation of the compounds. This work was financially supported by The Canon Foundation and KAKENHI (grant numbers 20H02756 and 18H04516) from the Japan Society for the Promotion of Science (JSPS).

Notes and references

1 N. Roy, B. Bruchmann and J. M. Lehn, *Chem. Soc. Rev.*, 2015, **44**, 3786–3807.
2 T. Maeda, H. Otsuka, A. Takahara, *Prog. Polym. Sci.*, 2009, **34**, 581–604.
3 P. Chakma, D. Konkolewicz, *Angew. Chem., Int. Ed.*, 2019, **58**, 9682–9695.
4 A. J. R. Amaral, G. Pasparakis, *Polym. Chem.*, 2017, **8**, 6464–6484.
5 C. Zhu, C. Ninh, C. J. Bettinger, *Biomacromolecules*, 2014, **15**, 3474–3494.
6 H. Nie, N. S. Schauser, N. D. Dolinski, J. Hu, C. J. Hawker, R. A. Segalman, J. Read de Alaniz, *Angew. Chem., Int. Ed.*, 2020, **59**, 5123–5128.
7 H. Wang, C. N. Zhu, H. Zeng, X. Ji, T. Xie, X. Yan, Z. L. Wu, F. Huang, *Adv. Mater.*, 2019, **31**, 1807328.
8 C.-H. Li, C. Wang, C. Keplinger, J.-L. Zuo, L. Jin, Y. Sun, P. Zheng, Y. Cao, F. Lissel, C. Linder, X.-Z. You, Z. Bao, *Nat. Chem*. 2016, **8**, 618–624.
9 H. Zhou, M. Chen, Y. Liu, S. Wu, *Macromol. Rapid Commun.*, 2018, **39**, 1800372.
10 I. Teasdale, S. Theis, A. Iturmendi, M. Strobel, S. Hild, J. Jacak, P. Mayrhofer, U. Monkowius, *Chem. - Eur. J.*, 2019, **25**, 9851–9855.
11 S. Theis, A. Iturmendi, C. Gorsche, M. Orthofer, M. Lunzer, S. Baudis, A. Ovsianikov, R. Liska, U. Monkowius, I. Teasdale, *Angew. Chem., Int. Ed.*, 2017, **56**, 15857–15860.
12 M. Burnworth, L. Tang, J. R. Kumpfer, A. J. Duncan, F. L. Beyer, G. L. Fiore, S. J. Rowan, C. Weder, *Nature*, 2011, **472**, 334–337.
13 D. W. R. Balkenende, S. Coulibaly, S. Balog, Y. C. Simon, G. L. Fiore, C. Weder, *J. Am. Chem. Soc.*, 2014, **136**, 10493–10498.
14 Y. S. Kim, R. Tamate, A. M. Akimoto, R. Yoshida, *Mater. Horiz.*, 2017, **4**, 38–54.
15 A. Winter, U. S. Schubert, *Chem. Soc. Rev*., 2016, **45**, 5311-5357.
16 K. Naskar, A. Dey, S. Maity, P. P. Ray, P. Ghosh, C. Sinha, *Inorg. Chem.*, 2020, **59**, 5518–5528.
17 S. R. Batten, N. R. Champness, X.-M. Chen, J. Garcia-Martinez, S. Kitagawa, L. Ö hrström, M. O'Keeffe, M. P. Suh, J. Reedijk, *CrystEngComm*, 2012, **14**, 3001–3004.
18 Y. Funasako, S. Mori, T. Mochida, *Chem. Commun*., 2016, **52**, 6277–6279.
19 R. Sumitani, H. Yoshikawa, T. Mochida, *Chem. Commun.*, 2020, **56**, 6189–6192.
20 R. Sumitani, T. Mochida, *Macromolecules*, 2020, **53**, 6968–6974.
21 T. Ueda, T. Tominaga, T. Mochida, K. Takahashi, S. Kimura, *Chem. Eur. J*., 2018, **24**, 9490–9493.
22 M. Kar, K. Matuszek, D. R. MacFarlane, *Ionic Liquids* in *Kirk–Othmer Encyclopedia of Chemical Technology*, Wiley, Hoboken, **2019**.
23 A. Komurasaki, Y. Funasako, T. Mochida, *Dalton Trans.*, 2015, **44**, 7595–7605.
24 B. Dietrich, M. W. Hosseini, J.-M. Lehn, R. B. Sessions, *Helv. Chim. Acta*, 1985, **68**, 289–299.
25 E. Badea, I. Blanco, G. D. Gatta. *J. Chem. Thermodyn.*, 2007, **39**, 1392–1398.
26 T. P. Gill, K. R. Mann, *Organometallics*, 1982, **1**, 485–488.
27 Y. Wang, K. Zaghib, A. Guerfi, F. F. C. Bazito, R. M. Torresi, J. R. Dahn, *Electrochim. Acta*, 2007, **52**, 6346–6352.
28 W. P. Cox, E. H. Merz, *J. Polymer Sci*., 1958, **28**, 619–622.
29 M. Galiński, A. Lewandowski, I. Stępniak, *Electrochim. Acta*, 2006, **51**, 5567–5580.
30 H. Tokuda, K. Hayamizu, K. Ishii, M. A. B. H. Susan, M. Watanabe, *J. Phys. Chem. B*, 2005, **109**, 6103–6110.
31 J. Rodrigues, M. G. Jardim, J. Figueira, M. Gouveia, H. Tomás, K. Rissanen, *New J. Chem.*, 2011, **35**, 1938–1943.

Graphical abstract

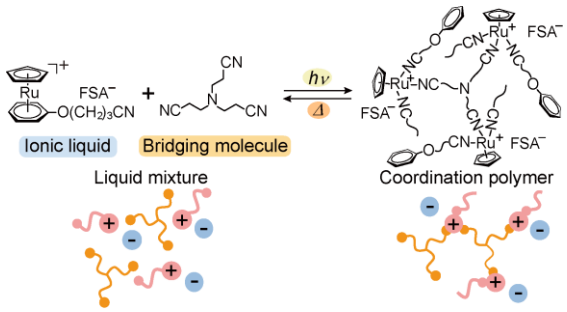

Liquid mixtures of a Ru-containing ionic liquid and bridging ligands were reversibly transformed into a coordination polymer or an oligomer liquid by the application of light and heat, thus enabling reversible control of their ionic conductivity.

Supporting Information

Reversible Formation of Soft Coordination Polymers from Liquid Mixtures of Photoreactive Organometallic Ionic Liquid and Bridging Molecules

Ryo Sumitani[a] and Tomoyuki Mochida*[a,b]

[a]*Department of Chemistry, Graduate School of Science, Kobe University, Rokkodai, Nada, Kobe, Hyogo 657-8501, Japan. E-mail: tmochida@platinum.kobe-u.ac.jp*

[b]*Center for Membrane and Film Technology, Kobe University, Rokkodai, Nada, Kobe, Hyogo 657-8501, Japan*

Contents

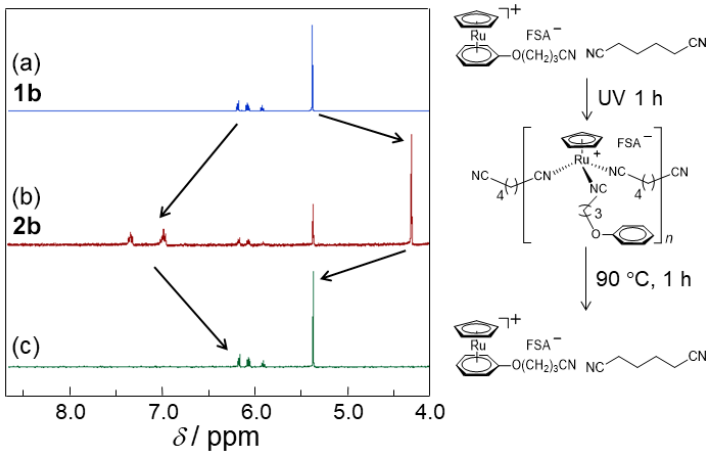

Fig. S1. ^{1}H NMR spectra of (a) **1b**, (b) **2b** (UV photoirradiated for 1 h), and (c) after heating **2b** at 90 °C for 1 h (solvent: CD_3CN).

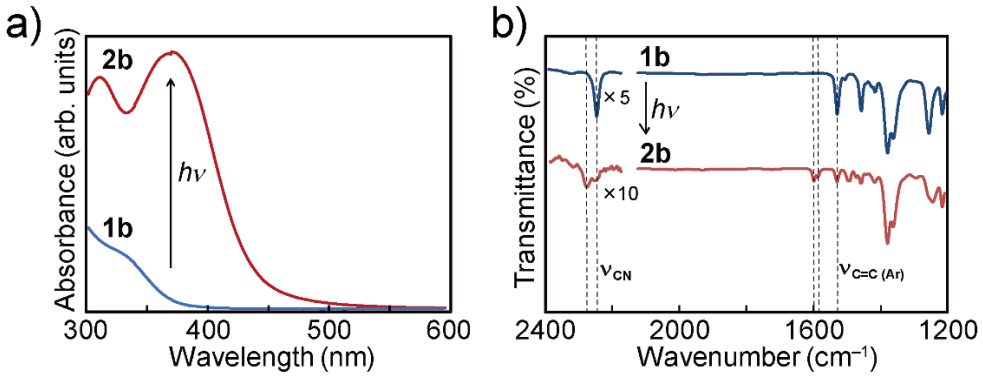

Fig. S2. (a) UV-vis spectra and (b) FT-IR spectra of **1b** and **2b** (UV photoirradiated for 1 h) and after heating **2b** at 90 °C for 1 h.

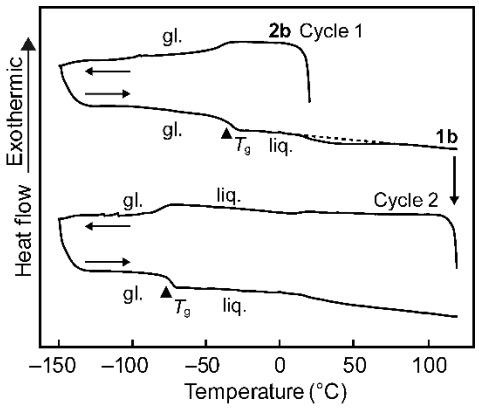

Fig. S3. DSC traces of **2b** (gl: glassy phase, liq: liquid phase). Dotted line shows the baseline.